MICROCOPY RESOLUTION TEST CHART
NATIONAL BUREAU OF STANDARDS-1963-A

AD-A154 143

OFFICE OF NAVAL RESEARCH

Contract N00014-80-C-0472

Task No. NR 056-749

TECHNICAL REPORT No. 66

Perturbative Treatment of Quasi-Resonant Proton
Neutralization at Alkali-Halide Surfaces

by

Franco Battaglia, Thomas F. George and Armando Lanaro

Prepared for Publication

in

Surface Science

Department of Chemistry
University of Rochester
Rochester, New York 14627

April 1985

OTIC FILE COPY

DTIC
ELECTE
MAY 24 1985
B

REPORT DOCUMENTATION PAGE

1a. REPORT SECURITY CLASSIFICATION Unclassified			1b. RESTRICTIVE MARKINGS		
2a. SECURITY CLASSIFICATION AUTHORITY			3. DISTRIBUTION/AVAILABILITY OF REPORT Approved for public release; distribution unlimited		
2b. DECLASSIFICATION/DOWNGRADING SCHEDULE					
4. PERFORMING ORGANIZATION REPORT NUMBER(S) UROCHESTER/DC/85/TR-66			5. MONITORING ORGANIZATION REPORT NUMBER(S)		
6a. NAME OF PERFORMING ORGANIZATION Department of Chemistry University of Rochester	6b. OFFICE SYMBOL (If applicable)		7a. NAME OF MONITORING ORGANIZATION Office of Naval Research (Code 413)		
6c. ADDRESS (City, State and ZIP Code) River Station Rochester, New York 14627			7b. ADDRESS (City, State and ZIP Code) Chemistry Program 800 N. Quincy Street Arlington, Virginia 22217		
8a. NAME OF FUNDING/SPONSORING ORGANIZATION Office of Naval Research	8b. OFFICE SYMBOL (If applicable)		9. PROCUREMENT INSTRUMENT IDENTIFICATION NUMBER Contract N00014-80-C-0472		
8c. ADDRESS (City, State and ZIP Code) Chemistry Program 800 N. Quincy Street Arlington, Virginia 22217			10. SOURCE OF FUNDING NOS.		

PROGRAM ELEMENT NO. 61153N	PROJECT NO. 013-08	TASK NO. NR 056-749	WORK UNIT NO.

11. TITLE
Perturbative Treatment of Quasi-Resonant Proton Neutralization at Alkali-Halide Surfaces

12. PERSONAL AUTHOR(S)
Franco Battaglia, Thomas F. George and Armando Lanaro

13a. TYPE OF REPORT Interim Technical	13b. TIME COVERED FROM _____ TO _____	14. DATE OF REPORT (Yr., Mo., Day) April 1985	15. PAGE COUNT 33

16. SUPPLEMENTARY NOTATION

Prepared for publication in Surface Science

17.	COSATI CODES		18. SUBJECT TERMS (Continue on reverse if necessary and identify by block number)
FIELD	GROUP	SUB. GR.	PROTON NEUTRALIZATION PERTURBATIVE TREATMENT
			ALKALI-HALIDE SURFACES FANO-ANDERSON POTENTIAL
			QUASI-RESONANT VALENCE BAND OF SOLID

19. ABSTRACT (Continue on reverse if necessary and identify by block number) A theoretical investigation of proton scattering from several alkali-halide surfaces is presented. These systems are suitable for a perturbative treatment since no hydrogenic atomic shell is embedded in the valence band of the solid where the neutralizing electron originates, which is a necessary condition for fast convergence of the perturbative expansion for the neutralization probability. The perturbative interaction is modeled by a Fano-Anderson effective potential, and the dependence of the results on the properties of the systems (namely, the width of the valence band of the solid and its position relative to the discrete atomic level) and on the dynamics of the process (determined here by a single parameter which controls the duration of the interaction, i.e., the collision energy) are critically discussed.

20. DISTRIBUTION/AVAILABILITY OF ABSTRACT UNCLASSIFIED/UNLIMITED ☒ SAME AS RPT. ☒ DTIC USERS ☐	21. ABSTRACT SECURITY CLASSIFICATION Unclassified	
22a. NAME OF RESPONSIBLE INDIVIDUAL Dr. David L. Nelson	22b. TELEPHONE NUMBER (Include Area Code) (202)696-4410	22c. OFFICE SYMBOL

PERTURBATIVE TREATMENT OF QUASI-RESONANT PROTON

NEUTRALIZATION AT ALKALI-HALIDE SURFACES

Franco Battaglia* and Thomas F. George
Department of Chemistry
University of Rochester
Rochester, New York 14627, USA

Armando Lanaro
Department of Physics
University of Rochester
Rochester, New York 14627, USA

Abstract

A theoretical investigation of proton neutralization by proton scattering from several alkali-halide surfaces is presented. These systems are suitable for a perturbative treatment since no hydrogenic atomic shell is embedded in the valence band of the solid where the neutralizing electron originates, which is a necessary condition for fast convergence of the perturbative expansion for the neutralization probability. The perturbative interaction is modeled by a Fano-Anderson effective potential, and the dependence of the results on the properties of the systems (namely, the width of the valence band of the solid and its position relative to the discrete atomic level) and on the dynamics of the process (determined here by a single parameter which controls the duration of the interaction, i.e., the collision energy) are critically discussed.

* Permanent address: Dipartimento di Scienze e Tecnologie Chimiche
II Universita' Delgi di di Roma
Via Orazio Raimondo - 00173 Roma
Italy
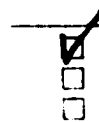
I. Introduction

Charge-exchange processes arising from monoenergetic ion beams scattered from solid surfaces have recently been the subject of much experimental[2-4] and theoretical[5-14] interest. When an ion impinges on a surface, a multiplicity of events are often involved, of which ion neutralization is perhaps one of the most studied. In fact, the creation of excited atomic states by transmission of energetic ions through thin foils and by reflection on surfaces has important applications in beam-foil spectroscopy[14-16] and in the chemical analysis of surfaces.[17] The majority of theoretical work has been based on the Fano-Anderson effective Hamiltonian introduced simultaneously by Anderson[18] and by Fano,[19] who applied it to solid-state physics problems and to the study of atomic spectra, respectively. Subsequently, the Fano-Anderson model has been applied by Newns[20] in the study of chemisorption on metals and recently has been used by other authors[7-14] mainly in connection with charge-exchange processes at surfaces.

In a previous paper (hereafter called Paper I),[13] we have applied the Fano-Anderson effective Hamiltonian to the problem of neutralization of positive ions scattered from surfaces and have given, using diagrammatic techniques, a perturbative expansion of the reduced density matrix elements of the neutralized atom. In I, we had carefully analyzed the validity of the first-order approximation and have found that its contribution to the neutralization probability is found to be dominant provided: (i) the discrete level of the atomic projectile is not embedded in the continuum of the valence band of the solid, and (ii) the duration of the interaction is sufficiently short, i.e., the collision energy is high enough.

In the present paper, we want to present calculations for a series of systems for which the requirement (1) is fulfilled, namely, hydrogen ions on alkali-halide surfaces. From Fig. 1, in which the relative position between the valence band of the alkali-halides and the hydrogenic level structure is depicted, we see that the first requirement is always fulfilled (except for LiF in whose valence band the ground level of hydrogen atom is embedded). We shall see that, in agreement with our results of paper I, calculations beyond first order are redundant for all the cases except for the neutralization of H^+ into the ground state of H from LiF surfaces. For all other cases, we present a comparison among the various systems, pointing out how the neutralization probability depends on the valence band width of the solid, where the neutralizing electron originates, and on the position of the atomic level relative to that band. Before presenting and discussing our results, we shall give in the following paragraph a brief summary of the theory whose details might be found in paper I.

II. Theory

Let us consider the experimental situation in which the following process occurs: an ion H^+ is sent against the surface of a solid S detaching from it one electron,

$$H^+ + S \longrightarrow H^* + S^+ . \tag{1}$$

The asterisk signifies that the atom H can be formed, in general, in an excited state. The collision times, usually around 10^{-15} sec, are orders of magnitude less than the lattice vibration period. Therefore, the surface does not have time to respond collectively, and the picture reduces to a many-interacting-electron problem, whose most convenient treatment is provided by the formalism

of second quantization. Moreover, since atomic radiative lifetimes, on order of 10^{-8} sec, are much longer than the collision times, here we need not be concerned with radiative de-excitation of possible excited atomic states during the collision, and we can treat the Process (1) separately from any radiative decay process of atom H^*.

The total Hamiltonian is:

$$H(t) = \sum_d \epsilon_d \, p_d^\dagger \, p_d + \sum_k \epsilon_k - \sum_k \epsilon_k \, h_k^\dagger \, h_k + H_I(t) \, , \qquad (2)$$

where $p_d^\dagger$ is an electron creation operator into the discrete state $|d\rangle$ of energy ϵ_d of the hydrogen atom, and $h_k^\dagger$ is a hole creation operator into the state $|k\rangle$ of energy ϵ_k of the valence band of the solid. The Fano-Anderson[21] time-dependent effective interaction is:

$$H_I(t) = \sum_{kd} \{ V_{kd}(t) \, h_k \, p_d + V_{kd}^*(t) \, p_d^\dagger \, h_k^\dagger \}. \qquad (3)$$

We shall restrict ourselves to a single band and single energy level interaction, whereby the only non-zero interaction is between the states of the valence band of the solid (whose lower and upper edges are ϵ_L and ϵ_U, respectively) and one (possibly degenerate) empty level (of energy ϵ) of H. Moreover, we assume that[7]

$$V_{kd}(t) = e^{-\lambda |t|} V_k \, , \qquad (4)$$

where λ is a parameter measuring the duration of the interaction, i.e., the collision energy of the incoming ion, and V_k a real parameter independent of the state $|d\rangle$.

The maximum amount of information on a quantum-mechanical system is given by the eigenvalues of a complete set of commuting observables, and the state of the system is specified by a vector of a suitable Hilbert space. If the specified observables do not form a complete set, the state of the system is described by its statistical operator ρ. A typical situation in which a physical system is not completely specified occurs when we want to describe it after it has interacted with an unobserved system. In this case the system of interest is specified by a reduced density operator.[22] The reduced density operator elements of the hydrogen atom which, subjected to the interaction (3), has been neutralized according to the process (1), are[13]

$$\langle d'|\rho^{(H)}(t)|d''\rangle = \sum_k \left[\frac{\langle \Psi_o|p_{d'}(t)h_k(t)|\Psi_o\rangle\langle \Psi_o|h_k^\dagger(t)p_{d''}^\dagger(t)|\Psi_o\rangle}{|\langle \Psi_o|\Psi_o\rangle|^2}\right], \qquad (5)$$

where $|\Psi_o\rangle$ is the (unknown) interacting ground state of the whole system, i.e., a vector state belonging to the Hilbert space tensor product of the electronic Hilbert space of the solid times the electronic Hilbert space of the incoming atom. In (5), the vectors and operators are in the Heisenberg Picture, but for a perturbative treatment the Interaction Picture is more suitable because the matrix elements are written in terms of the (known) non-interacting ground vacuum state $|0\rangle$,[23]

$$\frac{\langle \Psi_o|p(\infty)h_k(\infty)|\Psi_o\rangle}{\langle \Psi_o|\Psi_o\rangle} =$$

$$= \frac{\langle 0|T \exp\{-i \int_{-\infty}^{\infty} dt'\, e^{-\lambda|t'|}\, [ph_k\,\tilde{V}(t')]\}|0\rangle}{\langle 0|T \exp\{-i \int_{-\infty}^{\infty} dt'\, e^{-\lambda|t'|}\,\tilde{V}(t')\}|0\rangle}, \qquad (6)$$

where T is the time-ordering operator, and the tilde denotes the Interaction Picture. In I, we have given a diagrammatic treatment by which we have shown that, applying Wick's theorem,[24] the charge-transfer probability (assumed to be

independent of orbital and magnetic quantum numbers) into the atomic level of energy ϵ and degeneracy D is given by

$$P = 4\pi^2 D \sum_k \left| \sum_{n=0}^{\infty} f^{(2n+1)}(k) \right|^2 , \tag{7}$$

where the $(2n+1)$-th term of the sum is written according to the following rules:

1) Draw the $(2n+1)$-th diagram. It will have $2n+1$ dots, 2 external lines and $2n$ internal lines; $n+1$ are particle lines and $n+1$ are hole lines.

2) Number the dots from 1 to $2n+1$ so that the first and the $(2n+1)$-th have, respectively, a hole line and a particle line coming out of them. For example the fifth-order diagram is
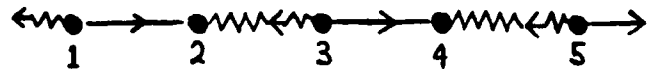
3) Write for each internal particle line connecting the dots j and $j+1$ a factor

$$\frac{1}{\omega_j + i\eta} \ \frac{1}{\lambda^2 + [\omega_{j+1} + \omega_j - (\epsilon_{k_j} - \epsilon)]^2} ,$$

and for each internal hole line connecting the dots j and $j+1$

$$\frac{1}{\omega_j + i\eta} \ \frac{\delta_{k_j k_{j+1}}}{\lambda^2 + [\omega_{j+1} + \omega_j - (\epsilon_{k_j} - \epsilon)]^2} .$$

4) For the two external lines write

$$\frac{\delta_{kk_1}}{\lambda^2+[\omega_1-(\epsilon_{k_1}-\epsilon)]^2}\frac{1}{\lambda^2+[\omega_{2n}-(\epsilon_{k_{2n+1}}-\epsilon)]^2} \qquad \text{if} \qquad n<0 \ ,$$

$$\frac{\delta_{kk_1}}{\lambda^2+(\epsilon_{k_1}-\epsilon)^2} \qquad\qquad \text{if} \qquad n=0 \ .$$

5) Write for the j-th dot a factor $\dfrac{i\lambda}{\pi}V_{k_j}$.

6) Integrate over all omegas, $\omega_1\ldots\omega_{2n}$, and sum over all k_j's, $k_1\ldots k_{2n+1}$.

In Table I is shown the correspondence between the elements of each diagram of the perturbative expansion and the analytical expression belonging to it. The relevant contractions of Table I are given by the following:

$$\tilde{h}_{k_\ell}(t_\ell)\ \tilde{h}^\dagger_{k_j}(t_j) = \delta_{k_\ell k_j}\ e^{i\epsilon_{k_\ell}(t_\ell-t_j)}\ \theta(t_\ell-t_j) \qquad (8a)$$

$$\tilde{h}_k\ \tilde{h}^\dagger_{k_j}(t_j) = \delta_{kk_j}\ e^{-i\epsilon_k t_j} \qquad (8b)$$

$$\tilde{p}(t_\ell)\ \tilde{p}^\dagger(t_j) = e^{-i\epsilon(t_\ell-t_j)}\ \theta(t_\ell-t_j) \qquad (8c)$$

$$p\ \tilde{p}^\dagger(t_j) = e^{i\epsilon t_j} \qquad (8d)$$

all other contractions = 0, $\qquad\qquad\qquad\qquad$ (8e)

where $\theta(t_1-t_2)$ is the Heaviside step function. The counting of topologically distinct diagrams[25] is particularly easy here: at each order n there is only one diagram which contributes n! times.

Making the substitution

$$\sum_k \longrightarrow \frac{\sqrt{2}}{\pi^2}\int_0^\Delta dE\ \sqrt{E} \ , \qquad (9)$$

where $\Delta = \epsilon_U - \epsilon_L$ is the valence band width, and in which the spin degeneracy of each $|k\rangle$ state has been taken into account, the first-order contribution to the neutralization probability is

$$P^{(1)}(\lambda,\epsilon) = \frac{4\sqrt{2}\ \lambda^2}{\pi^2} \int_0^\Delta dE \frac{\bar{V}^2(E)\ \sqrt{E}}{[\lambda^2 + (E-\epsilon)^2]^2}, \qquad (10)$$

where $\bar{V}(E) = V_{k(E)}$. The upper limit to the next contribution to the neutralization probability is given by

$$P^{(3)}(\lambda,\epsilon) = -\frac{\sqrt{2}}{\pi^2} \left\{ \alpha(\lambda,\epsilon) \int_0^\Delta dE \frac{(E-\epsilon)\bar{V}^2(E)\sqrt{E}}{[\lambda^2 + (E-\epsilon)^2]^2} \right.$$
$$\left. + \beta(\lambda,\epsilon) \int_0^\Delta dE \frac{\lambda^2\bar{V}^2(E)\sqrt{E}}{[\lambda^2 + (E-\epsilon)^2]^2} \right\} \qquad (11)$$

where

$$\alpha(\lambda,\epsilon) = \frac{\sqrt{2}}{\pi^2} \int_0^\Delta dE \frac{\bar{V}(E)\ \sqrt{E}[(E-\epsilon)^3 + 7\lambda^2(E-\epsilon)]}{[\lambda^2 + (E-\epsilon)^2]^2} \qquad (12)$$

and

$$\beta(\lambda,\epsilon) = \frac{\sqrt{2}}{\pi^2} \int_0^\Delta dE \frac{\bar{V}(E)\ \sqrt{E}\ [2(E-\epsilon)^2 - 4\lambda^2]}{[\lambda^2 + (E-\epsilon)^2]^2}. \qquad (13)$$

III. Calculations and Discussion

We model the scattering from alkali-halide surfaces of H^+, for
which the atomic energy levels are given by the usual Rydberg formula
and whose position is assumed to be preserved
during the scattering process. We also observe that conservation of energy would
require that the λ parameter, which controls the ion kinetic energy, changes after
the collision. However, although this would be a trivial extension, we do not
include it here because in the usual experimental situation $\Delta\lambda/\lambda \ll 1$, that is, the
energy exchanges are several orders of magnitude less than the ion kinetic energy.
It is also clear from Eq.(9) that the electrons in the valence band of the solid
have been considered "free". At the present, we are interested in exploring
the following general features of the process: (1) its dependence on the position
of the atomic level relative to the valence band of the solid; (2) how the
neutralization probability varies with λ, the only parameter which controls
the dynamics of the process, in particular, the duration of the interaction;
(3) a qualitative comparison among the various alkali-halide systems, i.e., how
the neutralization probability changes within a group of the periodic table;
and (4) how important the valence bandwidth and the work function of the solid
(see Table II) are for the neutralization process. The function $\overline{V}(E)$ has been
considered constant in a previous work,[12,13] and the same will be done here.
We have chosen $\overline{V}(E) = \overline{V} = 0.1$ a.u., a reasonable value for the strength of the
interaction.

From Fig. 1 it is clear that, within the theory and approximations so
far presented, the alkali-halide systems are suitable for a first-order perturba-
tion calculation if the conclusions of our previous paper I are correct. We
have computed both the first- and the third-order contributions to the neutrali-
zation probability into the hydrogenic states of principal quantum number
n=1,2,3 and 4 for all the systems displayed in Fig. 1. Indeed, for all the

alkali-bromide surfaces the third-order contribution to the neutralization probability into all hydrogenic bound states is, in absolute value, several orders of magnitude less than the first order. This is also the case for the neutralization into the hydrogenic excited bound states from all the alkali-fluoride surfaces. The situation is different for the neutralization into the ground state from the NaF, KF and, especially, LiF surfaces: $P^{(3)}$ is smaller than $P^{(1)}$ for NaF and KF, but only by one or two orders of magnitude. Although the atomic ground state is very close to one edge of the band, it is not in resonance with any state of the valence band of the solids, so that the first-order perturbation approximation can still be safely applied. We also notice that Eq. (11) gives actually an upper limit for $|P^{(3)}|$. This means that if $P^{(3)}$ as computed is small in comparison with $P^{(1)}$, a fortiori it would be so if Eq.(11) were exact.

In Table III we display $P^{(1)}$ and $P^{(3)}$ as computed for Eqs.(10) and (11) as a function of λ for the neutralization into the hydrogenic ground state from the three alkali-fluoride systems considered. Clearly, for LiF where $|P^{(3)}|$ can be several orders of magnitude larger than $P^{(1)}$, the first-order perturbation approximation breaks down. We shall not pursue further the calculations for this case, but shall be concerned only with cases in which the first-order approximation is satisfactory. Therefore, the neutralization from the LiF surface will be studied only for the hydrogenic excited states. This is tantamount to assuming that electron capture from different atomic shells is uncorrelated. This is physically reasonable because the spatial extension of the atomic orbitals increases as the squares of the principal quantum number. Finally, from Table III we observe that the difference between the absolute values of $P^{(1)}$ and $P^{(3)}$ becomes greater as λ increases. This is easily understood in terms of the

physical meaning of the parameter λ: it represents the duration of the inter-action, and the shorter it is, the better the first-order perturbative approximation becomes, and at very large λ it applies even to the resonant case.

The neutralization probabilities into various bound states of the hydrogen atom as a function of λ for the alkali-fluoride and alkali-bromide surfaces are shown in Figs. 2 and 3, respectively, where two general features can be readily seen: the maxima of the neutralization probability and its rapid decrease for values of λ larger than the value where those maxima occur. We expect the interaction time to become smaller as λ increases, and therefore the electron to have less time to "jump" into the discrete atomic level. On the other hand, large λ can ease the resonance requirement because energy conservation can be violated for short-duration processes. Those two competing effects give rise to an optimal value at which the ionization probability reaches a maximum. The fact that in Figs. 2 and 3 the maxima occur at greater values of λ for greater values of principal quantum number n is also in agreement with what we have just mentioned: the smaller the value of n, the closer the atomic level is to the edges of the valence band, and the smaller is the value of λ at which those maxima occur given that the resonance requirement becomes less stringent.

The neutralization probability is seen to increase with increasing quantum number n. There are two competing effects: as n increases, the atomic level moves away from the valence band of the solid, which decreases the neutralization probability, but also the degeneracy of the n shell increases as n^2, giving more states available to the neutralizing electron. The effect of the degeneracy of the atomic states is more dominant than that of the separation in energy between the atomic states and the valence bands of the solids in all cases except for the ground-state neutralization from the NaF and KF surfaces. In Figs. 2(b) and 2(c) we see that the curves with n=1 are well above all the others, in

agreement with the proximity of the ground state to the valence bands of NaF

and KF (see Fig. 1). At greater values of λ, where the separation between

the atomic excited states and the solid valence band states has less effect

on the neutralization process, the degeneracy of these excited states becomes

more important, and the neutralization probability into the ground state is,

again, smaller than that into the excited states. This also explains why

the curves of Fig. 3 cross each other while the ones of Fig. 2 (except for n=1)

do not. The valence bands of the fluoride systems are so far away from the

atomic excited states which, in turn, are comparatively so close to each

other, that the quasi-resonant nature between the atomic states and the valence

bands does not change appreciably going from n=2 to n=4 (n=1, as we said, is

a special case). Therefore, the degeneracy increasing is, for all values of λ ,

the dominant effect. The situation is different for the bromide systems. Their

valence bands are located somewhere in between the n=1 and n=2 atomic shells.

Hence, in the region of values of λ where its increase can ease the resonant

structure between the atomic levels and the valence bands, the competition

between the resonant effect and the degeneracy effect is clearly seen by the

crossing of the curves in Fig. 3. At higher values of λ where the short

duration of the interaction makes the neutralization probability decrease with

increasing of λ , the degeneracy effect is the dominant one.

In Figs. 4 and 5, we compare, for a given atomic shell, the neutralization

probability as a function of λ for scattering from different surfaces. In Fig. 4

we show the neutralization probability into the ground state from the fluoride

surfaces [Fig. 4(b)]. The LiF curve is missing from Fig. 4(a) because a calcu-

lation more exact than the first-order approximation would be necessary to

determine it. The relative importance of the surface properties can be seen

here. The lower edge of the valence band of KF is closer to the atomic K shell than the one of NaF. Therefore, in the region of λ where the resonant effect is important, KF is more easily ionizable than NaF. However, at higher values of λ, the two curves cross each other, which is a manifestation of the larger bandwidth of NaF compared to the one of KF (see Fig. 1 and Table II). In Fig. 4(b) the neutralization probability follows the trend LiBr > NaBr > KBr for all values of λ. In this case, the resonant effect and the bandwidth effect both favor an easier ionization of LiBr than NaBr and of NaBr than KBr (see Fig. 1).

In Fig. 5 we show the neutralization probability into the L shell from fluoride surfaces [Fig. 5(a)] and from bromide surfaces [Fig. 5(b)]. From Fig. 5(a) we see that the curve relative to KF is always below the one relative to NaF: the bandwidth of NaF is larger and its upper band edge closer to the L atomic shell than the bandwidth and upper band edge of KF (see Fig. 1). The curve of LiF is above the other fluoride curves at large values of λ, where only the bandwidth effect determines the trend of the neutralization probability. However, as λ decreases, that curve crosses first the curve of NaF and then the curve of KF. This has to be so, given that the valence band of NaF is wider and its upper edge is closer than that for KF to the $n=2$ atomic energy level. The behavior of the neutralization probability curves into the shells with $n=3$ and $n=4$ not presented here is qualitatively similar, for both the fluoride and bromide systems, to the behavior of the curves shown for $n=2$. Only their quantitative behavior changes, and this has already been examined in Figs. 2 and 3.

IV. Conclusions

We have performed calculations of the neutralization probability of protons impinging on various alkali-halide surfaces. Due to the ease with which single

crystals of these ionic semiconductors may be grown, they should be hopefully very apt for experimental measurements. Moreover, they play an important role in our theory which has been summarized at the beginning of this paper and whose details might be found in paper I. In fact, their electronic structure is such that the width of their valence band and its locations in an energy scale do not allow any bound stationary state of the hydrogen atom to be in resonance with any stationary state of the valence electrons of the solid (with the exception of the ground state of the hydrogen which is indeed embedded into the continuum of the valence band of LiF). From the conclusions of paper I, this is a most favorable situation for the reliability of first-order perturbations calculations. Under those conditions we are therefore in a position of being able to explore how the neutralization probability depends on various properties of the systems considered. The decrease of the interaction time always plays a double role: it gives less time for a surface electron to "jump" into an atomic state but, also, enhances the resonance condition between the discrete atomic state and the continuum of the surface states. The increase of the atomic principal quantum number always enhances the neutralization probability due to the enhanced degeneracy of the energy levels. The proximity of an atomic state to the valence band always makes the neutralization into that state easier. Finally, the wider the valence band is, the easier the neutralization process occurs. It is the interplay of all these general rules that determines quantitatively the relative neutralization probability from valence bands of different systems into different atomic states.

Our main goal has been to gain a qualitative idea of the behavior of the neutralization probability as a function of all the above-mentioned properties.

Therefore, although the parameterization chosen is an oversimplification for any quantitative-type calculation, it suffices to give the qualitative features we are after. For example, if it were possible to have, by other means, a realistic analytic expression for the function V_{kd} [see Eq. (3)][14], λ would then be the only truly undetermined parameter, and its dependence on the collision energy could be determined by comparing the first order calculation with the neutralization probability experimentally measured at high collision energy.

References

1. A very good up-to-date review on the subject has been written by E. W. Thomas in Applied Atomic Collision Physics, Vol. 4, ed. by S. Datz (Academic Press, New York, 1983), pp. 299-326.

2. H. H. Brongersma and T. M. Buck, Surf. Sci. 53, 649 (1975).

3. R. L. Erickson and D. P. Smith, Phys. Rev. Lett. 34, 297 (1975).

4. E. G. Overbosch, B. Rasser, A. D. Tenner and J. Los, Surf. Sci. 92, 310 (1980).

5. A. Blandin, A. Nourtier and D. W. Hone, J. Physique 37, 369 (1976).

6. J. C. Tully, Phys. Rev. B 16, 4324 (1977).

7. W. Bloss and D. Hone, Surf. Sci. 72, 277 (1978).

8. G. Blaise and A. Nourtier, Surf. Sci. 90, 495 (1979).

9. Y. Muda and T. Hanawa, Surf. Sci. 97, 283 (1980).

10. R. Brako and D. M. Newns, Surf. Sci. 108, 253 (1981).

11. K. L. Sebastian, V. C. Jyothi Bhasu and T. B. Grimley, Surf. Sci. 110, L571 (1981).

12. K. S. Lam, K. C. Liu and T. F. George, Phys. Lett. 101A, 356 (1984); K. C. Liu, T. F. George and K. S. Lam, Solid State Comm. 53, 67 (1985).

13. F. Battaglia and T. F. George, J. Chem. Phys., in press.

14. R. Brako, Phys. Rev. B 30, 5629 (1984).

15. S. Bashkin, Beam-Foil Spectroscopy (Springer-Verlag, Heidelberg, 1976), pp. 5-32.

16. F. Battaglia and T. F. George, Nuovo Cimento D 3, 653 (1984).

17. T. M. Buck, in Methods and Phenomena 1: Methods of Surface Analysis, ed. by A. W. Czanderna (Elsevier, New York, 1975), pp. 75-103.

18. P. W. Anderson, Phys. Rev. 124, 41 (1961).

19. U. Fano, Phys. Rev. 124, 1866 (1961).

20. D. M. Newns, Phys. Rev. 178, 1123 (1969).

21. G. D. Mahan, Many-Particle Physics (Plenum, New York, 1981), p. 256.

22. U. Fano and J. H. Macek, Rev. Mod. Phys. 45, 553 (1973).

23. A. A. Abrikosov, L. P. Gorkov and I. E. Dzyaloshinski, Methods of Quantum Field Theory in Statistical Physics (Dover, New York, 1975), Chapter 2.

24. G. C. Wick, Phys. Rev. 80, 268 (1950).

25. F. Battaglia and T. F. George, J. Math. Phys. 25, 3489 (1984).

26. A. J. Dekker, Solid State Physics (Prentice-Hall, Englewood Cliffs, New Jersey, 1962), p. 371.

27. American Institute of Physics Handbook (McGraw-Hill, New York, 1972), Chapt. 9, p. 17.

Table I. Graphical representation of each contraction given by Eq. (8).

Analytical Expression | Graphical Representation
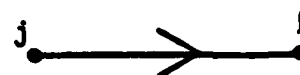
$$v_{k_j} e^{-\lambda |t_j|}$$

$$\tilde{h}_{k_\ell}(t_\ell)\, \tilde{h}^{+}_{k_j}(t_j)$$

$$h_k\, \tilde{h}^{+}_{k_j}(t_j)$$

$$\tilde{p}(t_\ell)\, \tilde{p}^{+}(t_j)$$

$$p\, \tilde{p}^{+}(t_j)$$

Table II. Work function and bandwidth in eV for the alkali-halide systems considered in the present paper. The data are taken from Refs. 26 and 27.

System	Work Function	Bandwidth
LiF	12.50	2.10
NaF	11.00	1.70
KF	11.40	1.50
LiBr	9.00	1.20
NaBr	8.20	0.75
KBr	8.30	0.55

Table III. First-order ($P^{(1)}$) and third-order ($P^{(3)}$) neutralization probabilities into the hydrogenic ground state from the alkali-fluoride surfaces as a function of λ. For NaF and KF, $|P^{(3)}|<|P^{(1)}|$ and the first-order calculations can be considered satisfactory. For LiF a more exact treatment is required. For all other cases not reported in this table (neutralization from the alkali-bromide surfaces and into hydrogenic excited states), $|P^{(3)}|<<|P^{(1)}|$.

	LiF		NaF		KF	
λ	$P^{(1)}$	$P^{(3)}$	$P^{(1)}$	$P^{(3)}$	$P^{(1)}$	$P^{(3)}$
5. −4*	.34 +1	.30 +3	.12 −5	−.29 −4	.23 −5	−.45 −4
1. −3	.17 +1	.77 +2	.48 −5	−.30 −4	.93 −5	−.48 −4
5. −3	.34	.35 +1	.12 −3	−.71 −4	.23 −3	−.14 −3
1. −2	.17	.96	.44 −3	−.17 −3	.81 −3	−.34 −3
5. −2	.24 −1	.27 −1	.33 −2	.10 −3	.41 −2	.36 −3
1. −1	.75 −2	.27 −2	.27 −2	.28 −3	.27 −2	.31 −3
5. −1	.33 −3	.53 −5	.23 −3	.26 −5	.19 −3	.18 −5
1.	.82 −4	.33 −6	.58 −4	.17 −6	.49 −4	.12 −6

* 5. −4 means 5. $\times 10^{-4}$

Figure Captions

Fig. 1. Electronic structure of the first four hydrogenic shells and of
the valence band of some alkali-halide solids. Notice that only LiF has
a discrete atomic state embedded in its valence band.

Fig. 2. Neutralization probabilities P into various hydrogenic shells from
the LiF (a), NaF (b) and KF (c) surfaces, as a function of log λ. P is
given by the sum $P^{(1)} + P^{(3)}$ [Eqs. (10) and (11)] even though there is
very little contribution from $P^{(3)}$ (see Table III). Notice that in (a)
the hydrogenic ground state (n=1) is missing: the neutralization into it
from LiF needs a more exact treatment. Notice also that the increase of
the atomic shell degeneracy is a more important factor in determining the
neutralization probability than the resonance factor, in all cases except
for the neutralization into the atomic ground state from the NaF (b) and
KF (c) surfaces.

Fig. 3. Neutralization probability P into various hydrogenic shells from
the LiBr (a), NaBr (b) and KBr (c) surfaces as a function of log λ. Again,
$P = P^{(1)} + P^{(3)}$ but now P is practically indistinguishable from $P^{(1)}$. Notice
the crossing of these curves due to the proximity of the alkali-bromide
valence bands to the excited atomic shells.

Fig. 4. Neutralization probability P into the hydrogenic ground state (n=1)
from the alkali-fluoride (a) and alkali-bromide (b) surfaces. In (b), the
resonance factor and the width of the valence bands both favor the trend
LiBr > NaBr > KBr for the ground-state neutralization probability (see
Fig. 1). In (a), the interplay between those two factors causes the crossing
of the curves as shown.

Fig. 5. Neutralization probability P into the first hydrogenic excited state
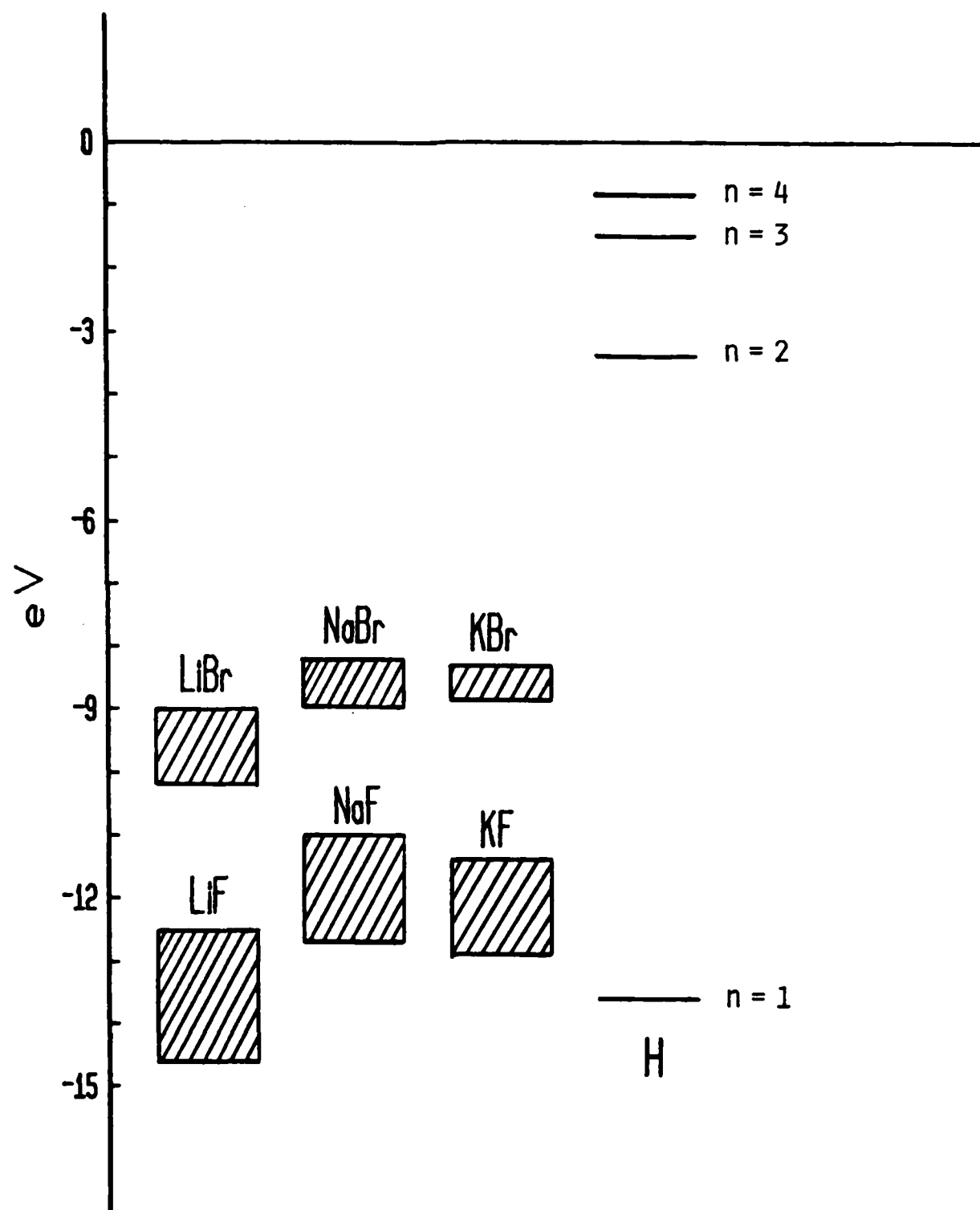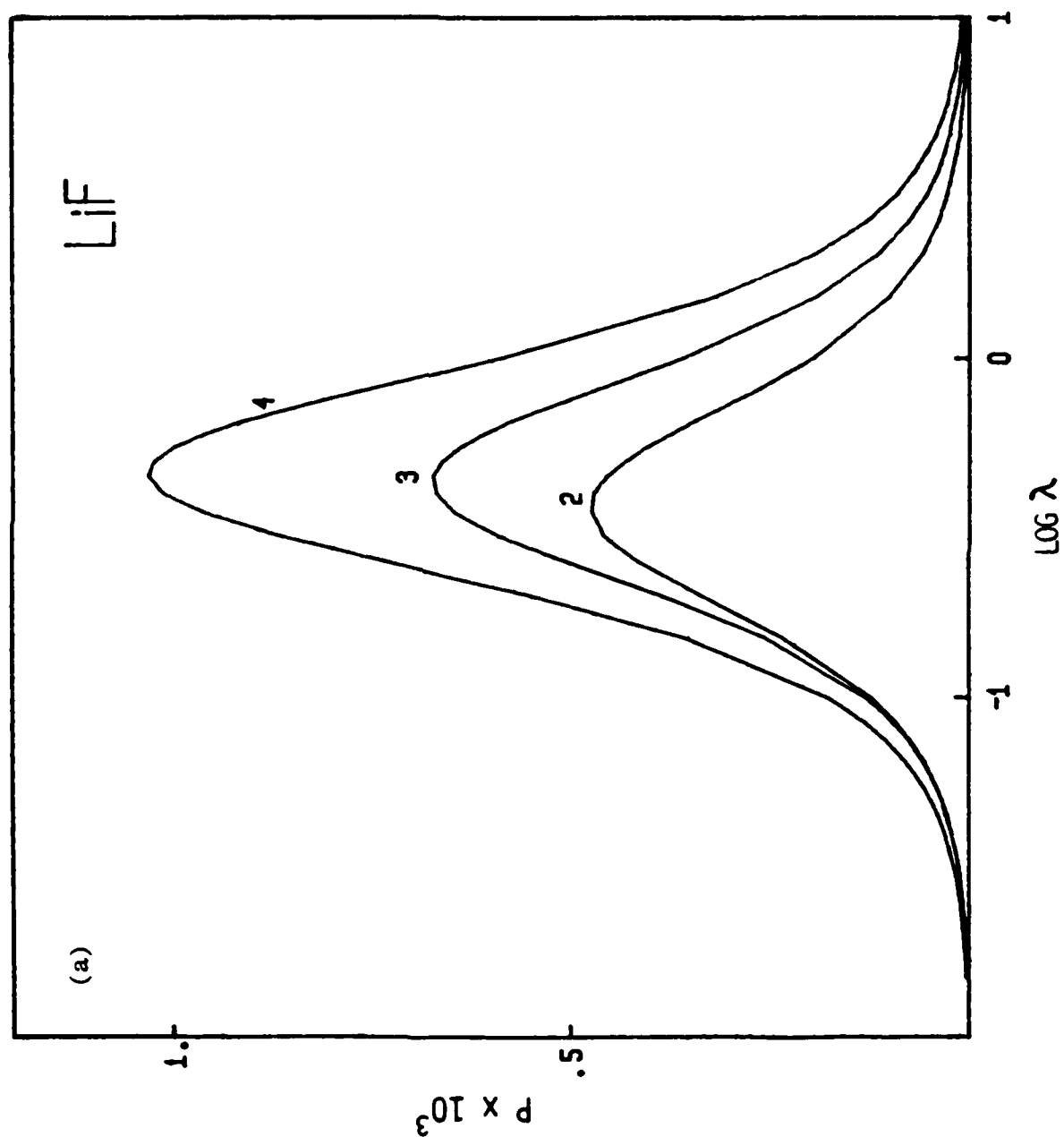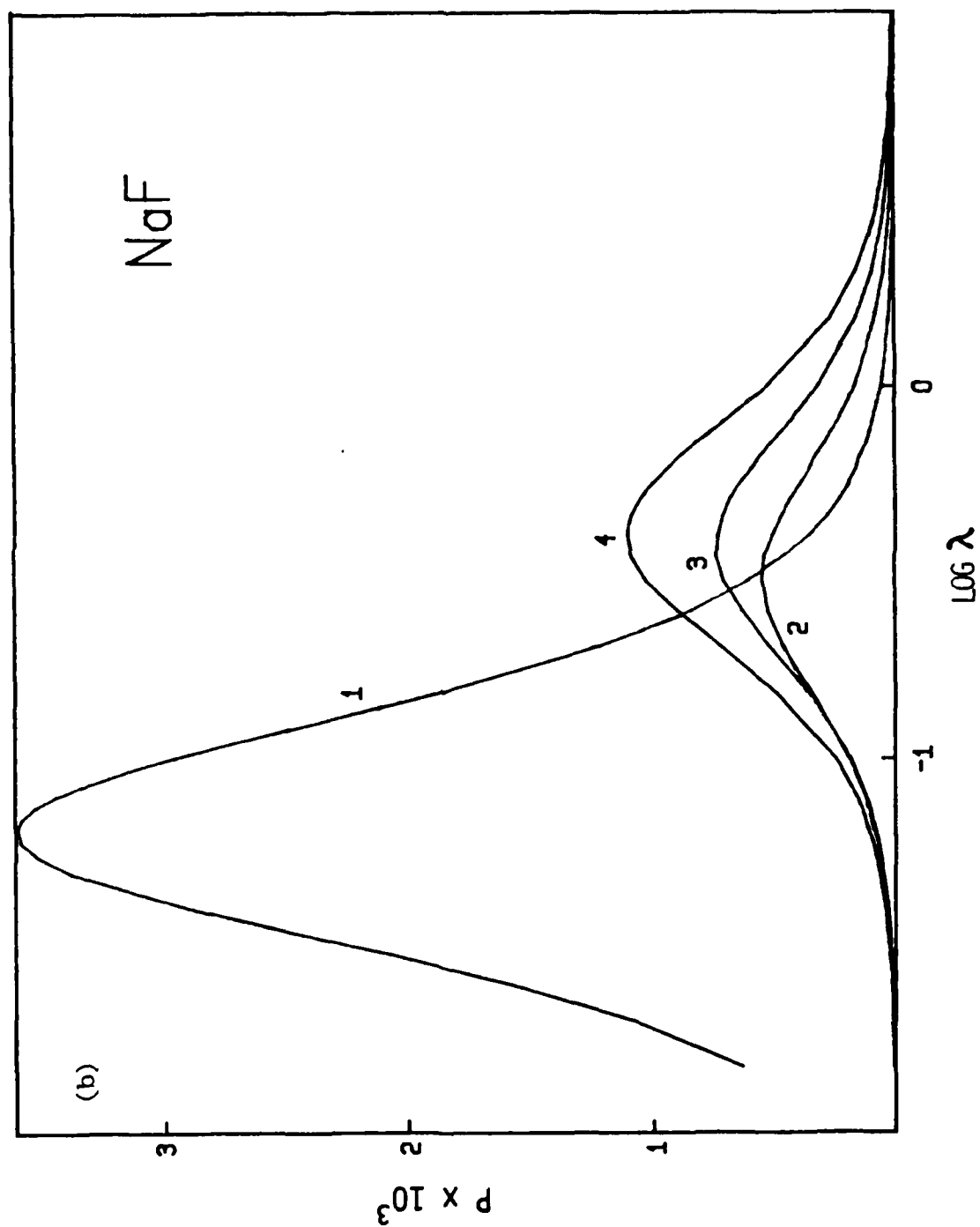(n=2) from the alkali-fluoride (a) and alkali-bromide (b) surfaces.
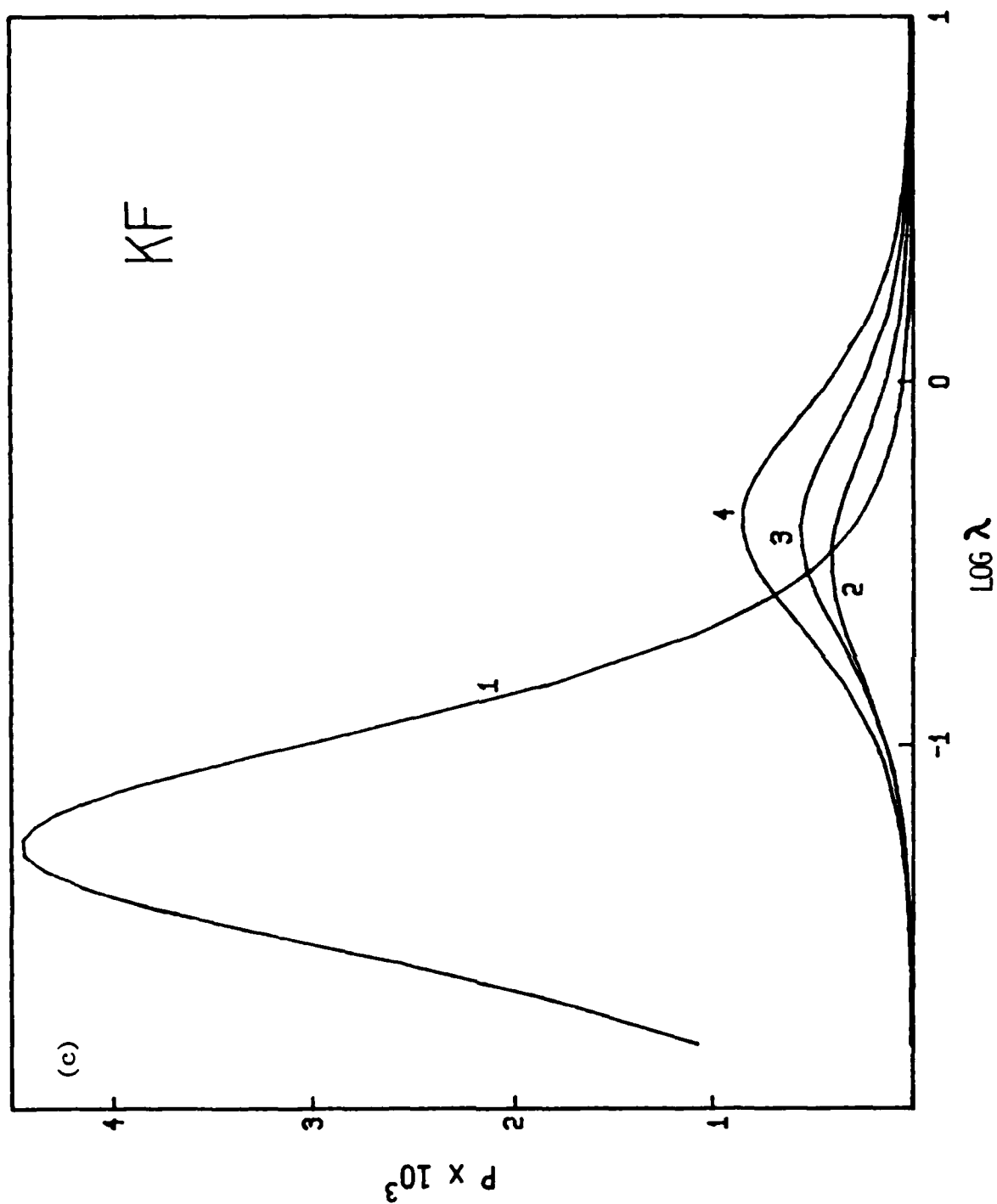
Fig. 1

Fig. 2

LiF

(a)

LOG λ

P X 10³

Fig. 2

(b) NaF

Fig. 2

(c) KF

Fig. 3

Fig. 3

(b) NaBr

Fig. 3

(c) KBr

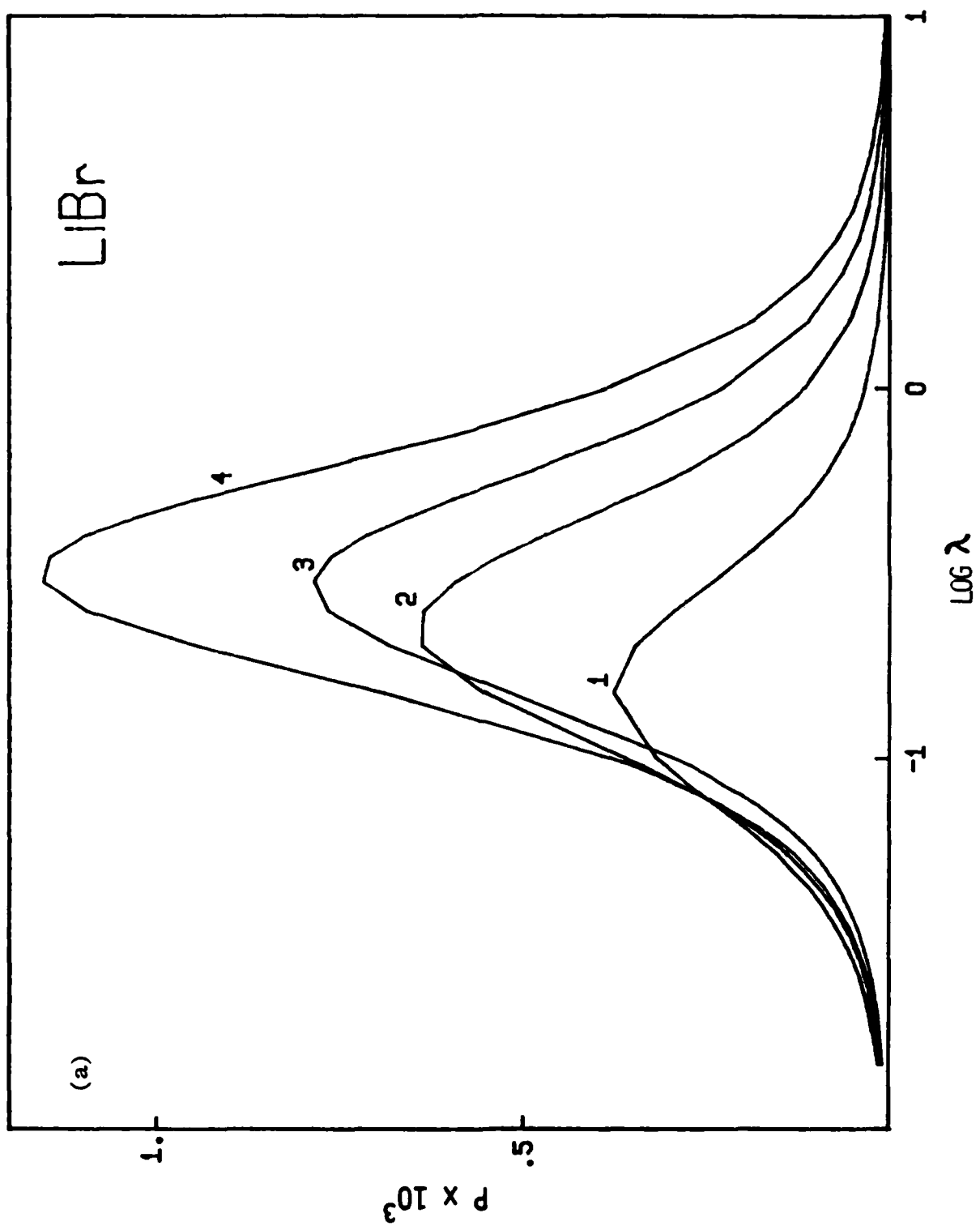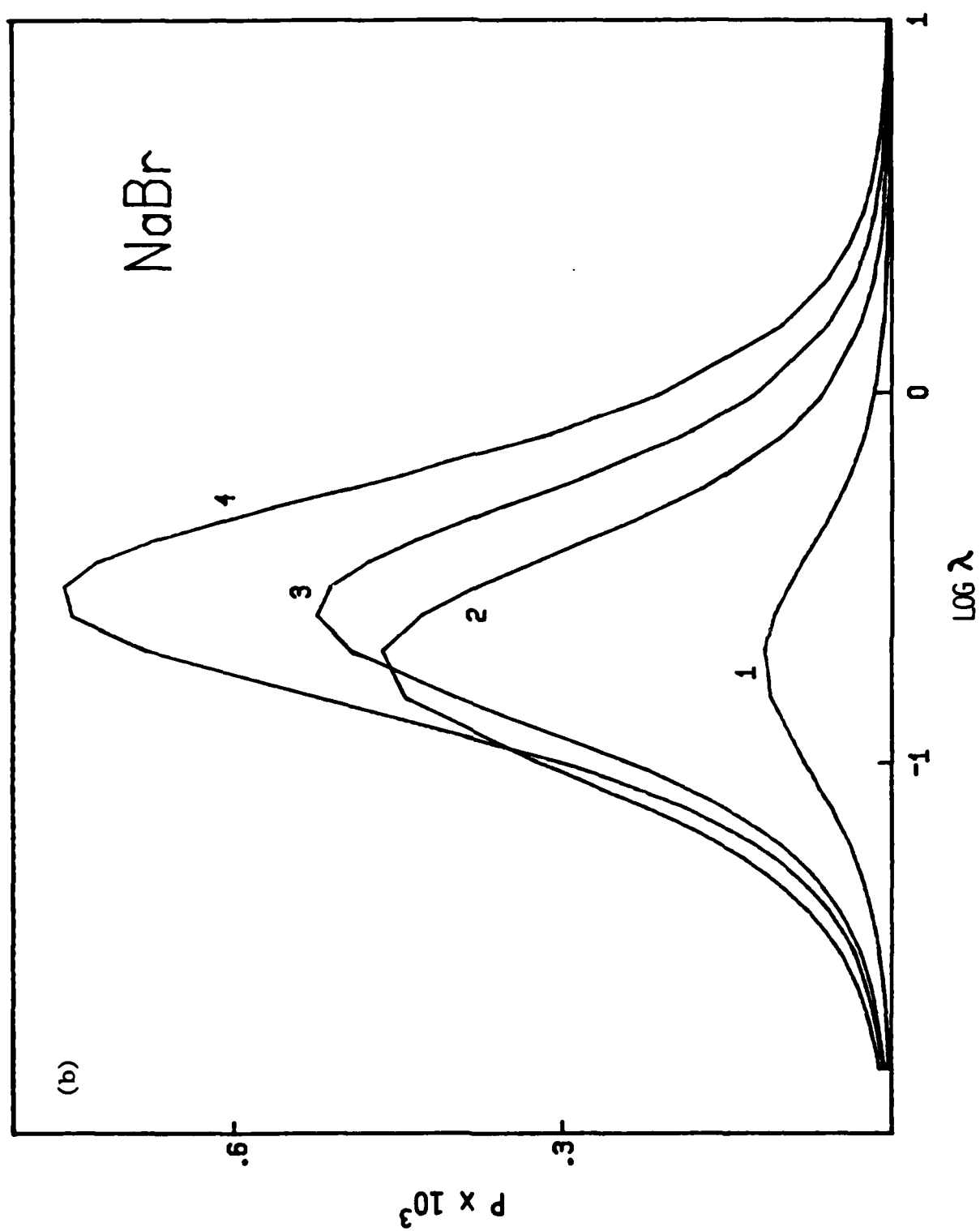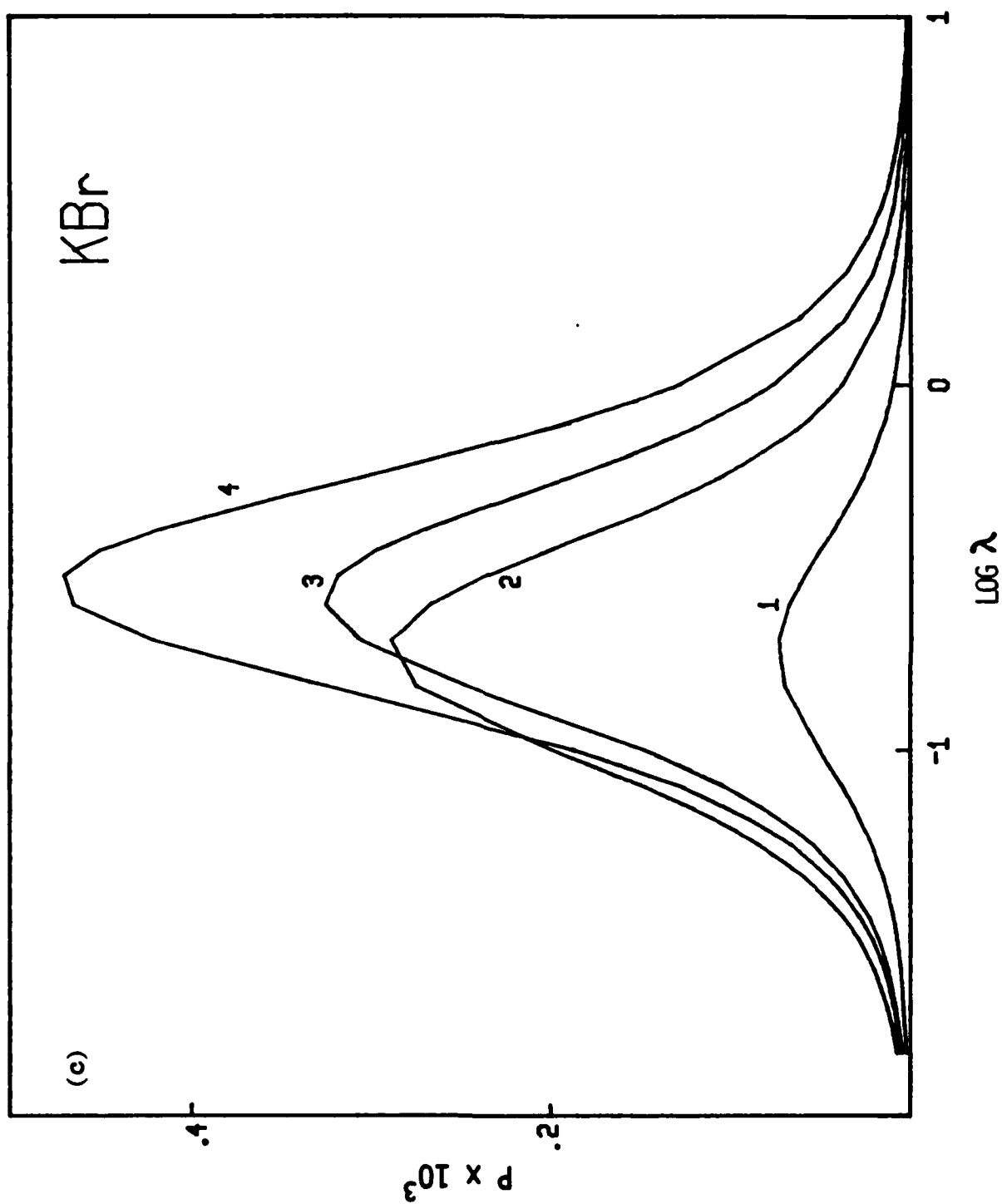Fig. 4

Fig. 4

Fig. 4

Fig. 5

Fig. 5 (a) n=2

Fig. 5

(b)

n=2

LOG λ

P X 10³
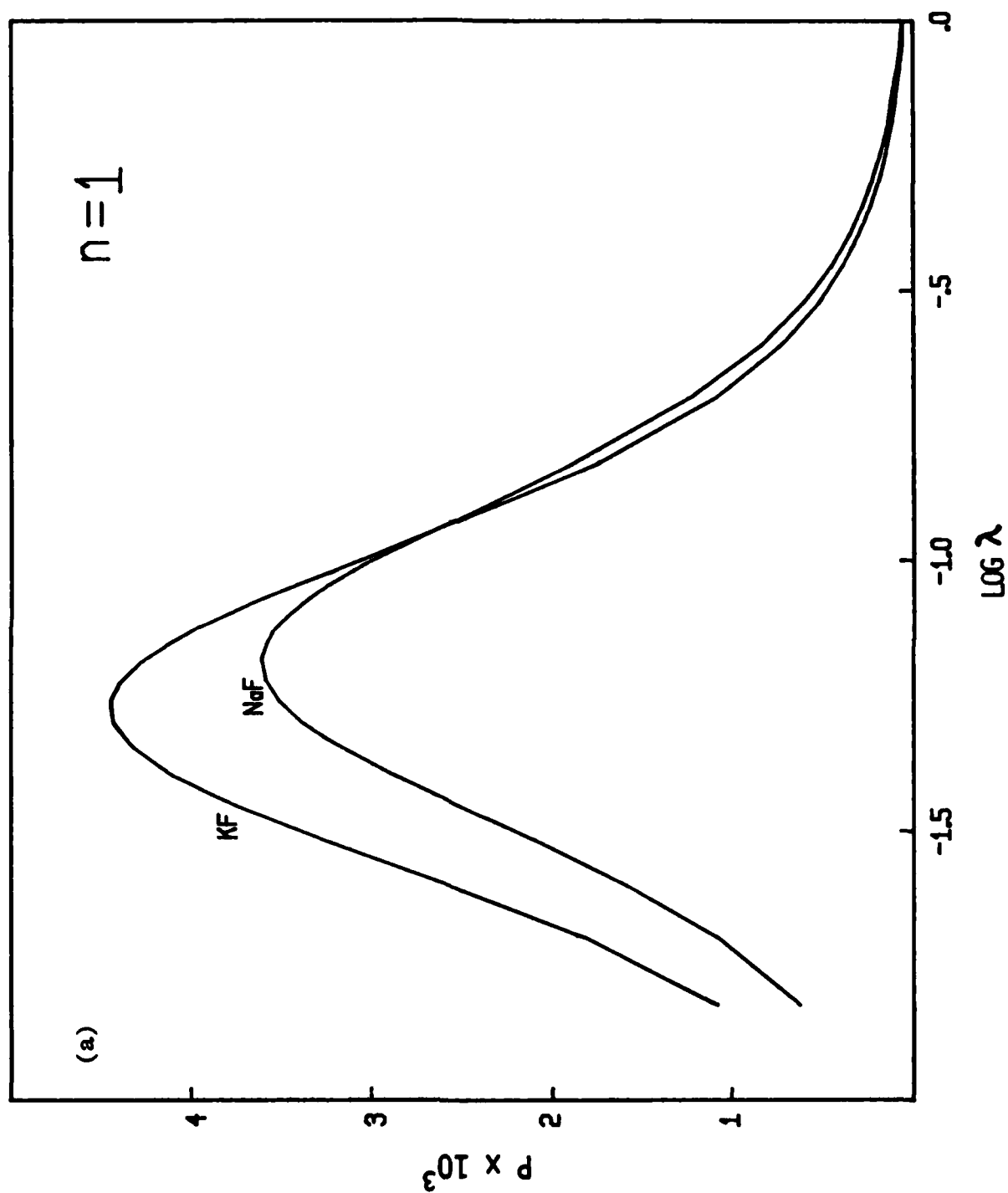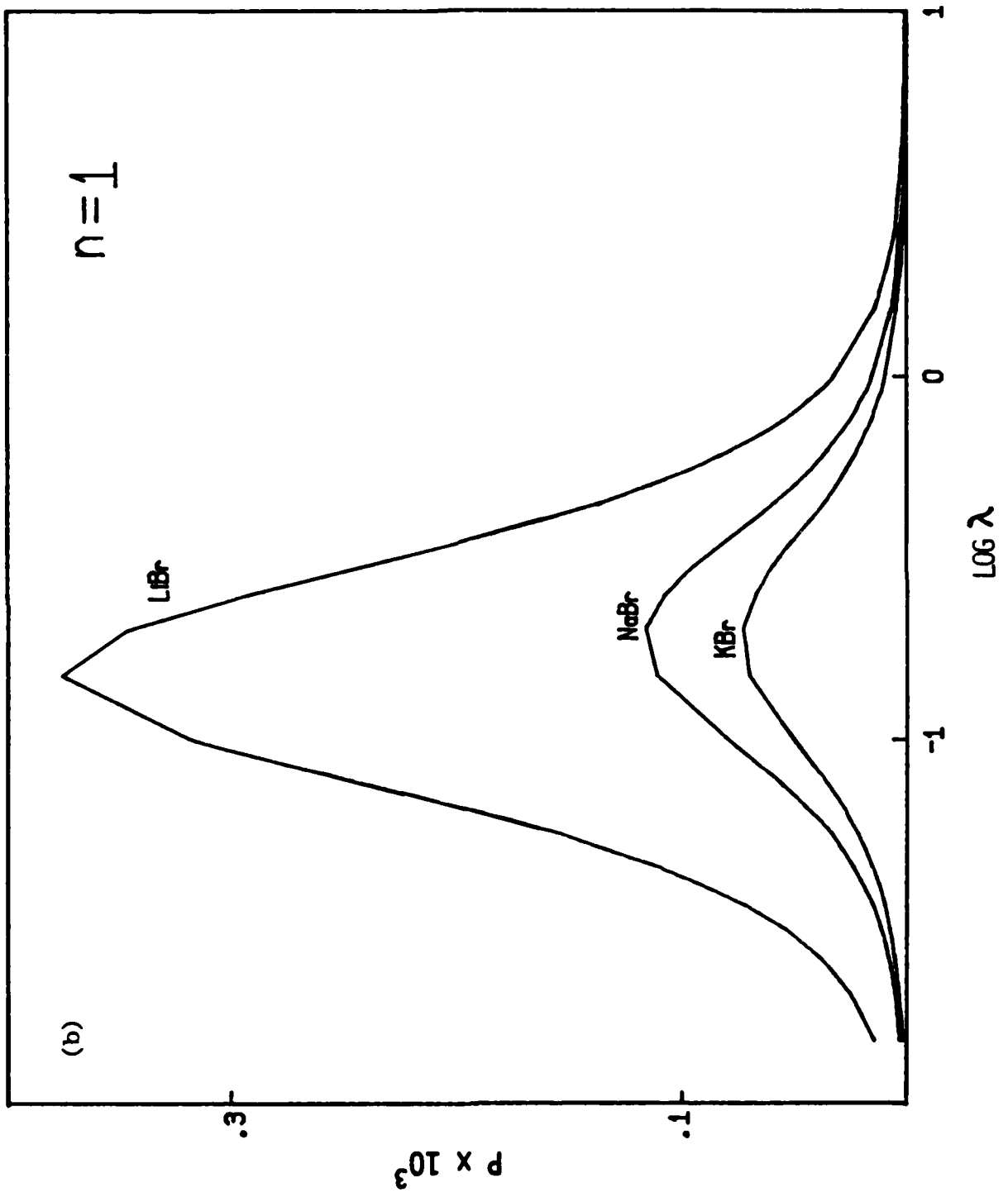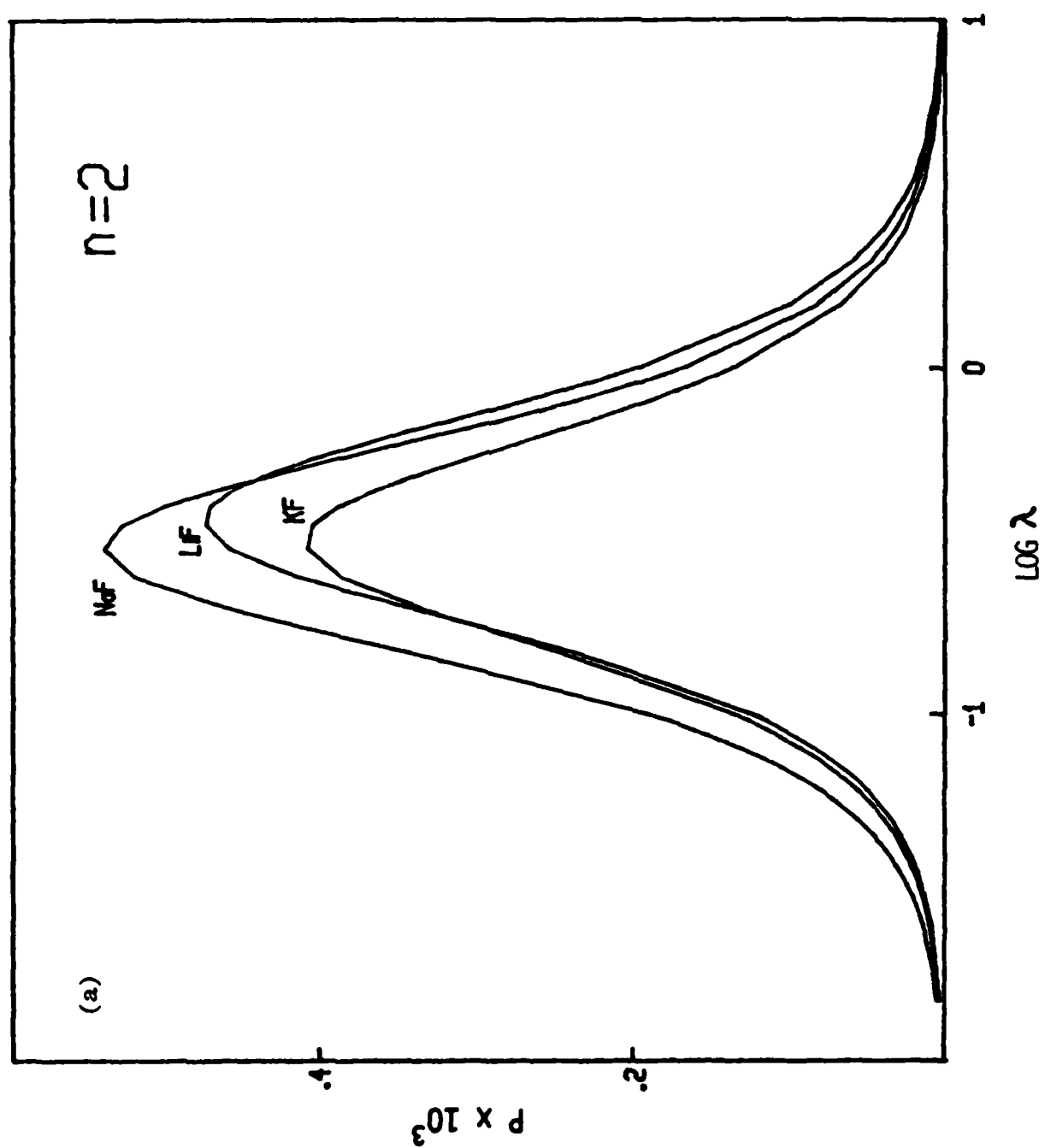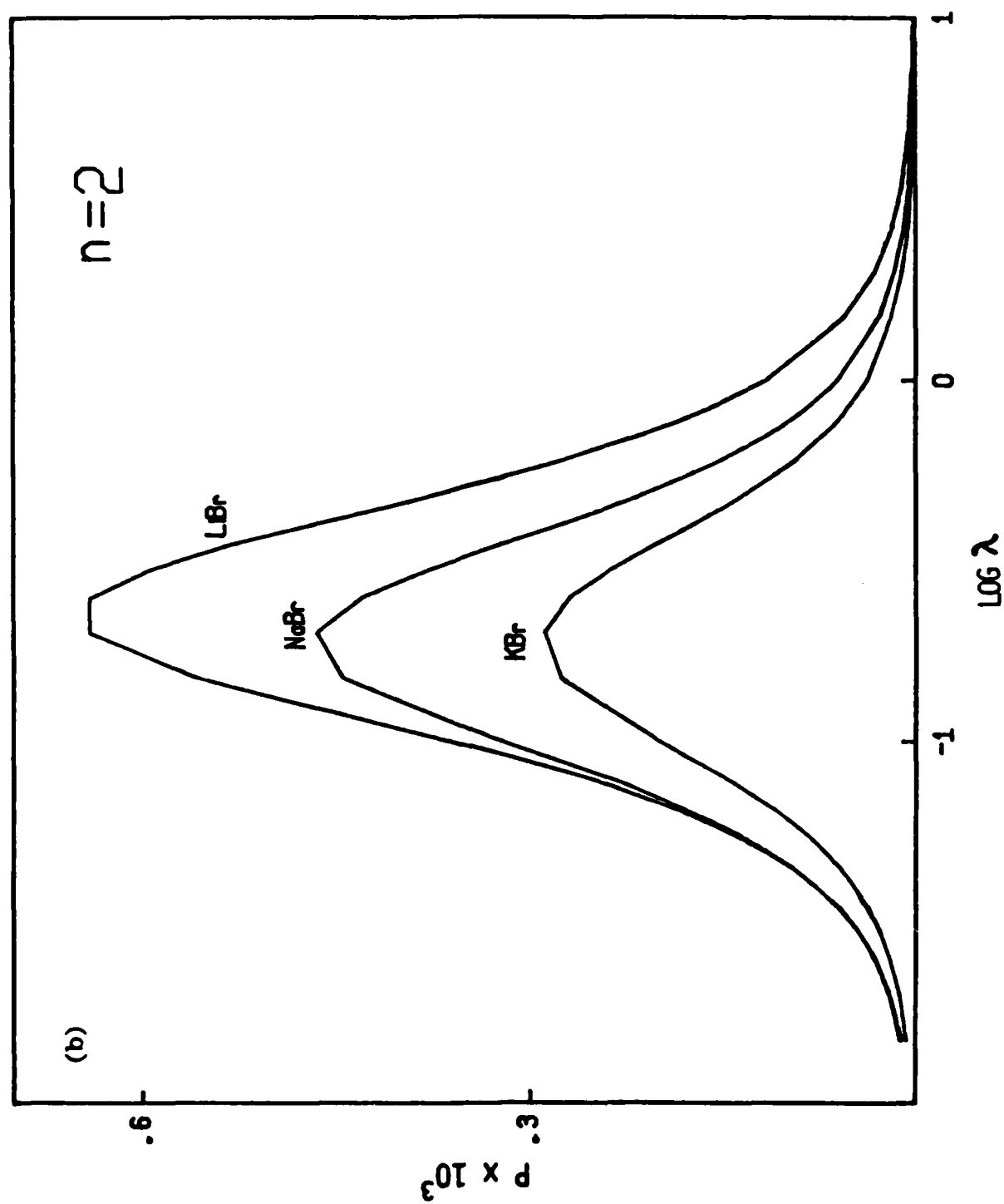
TECHNICAL REPORT DISTRIBUTION LIST, GEN

	No. Copies		No. Copies
Office of Naval Research Attn: Code 413 800 N. Quincy Street Arlington, Virginia 22217	2	Dr. David Young Code 334 NORDA NSTL, Mississippi 39529	1
Dr. Bernard Douda Naval Weapons Support Center Code 5042 Crane, Indiana 47522	1	Naval Weapons Center Attn: Dr. A. B. Amster Chemistry Division China Lake, California 93555	1
Commander, Naval Air Systems Command Attn: Code 310C (H. Rosenwasser) Washington, D.C. 20360	1	Scientific Advisor Commandant of the Marine Corps Code RD-1 Washington, D.C. 20380	1
Naval Civil Engineering Laboratory Attn: Dr. R. W. Drisko Port Hueneme, California 93401	1	U.S. Army Research Office Attn: CRD-AA-IP P.O. Box 12211 Research Triangle Park, NC 27709	1
Defense Technical Information Center Building 5, Cameron Station Alexandria, Virginia 22314	12	Mr. John Boyle Materials Branch Naval Ship Engineering Center Philadelphia, Pennsylvania 19112	1
DTNSRDC Attn: Dr. G. Bosmajian Applied Chemistry Division Annapolis, Maryland 21401	1	Naval Ocean Systems Center Attn: Dr. S. Yamamoto Marine Sciences Division San Diego, California 91232	1
Dr. William Tolles Superintendent Chemistry Division, Code 6100 Naval Research Laboratory Washington, D.C. 20375	1	Dr. David L. Nelson Chemistry Division Office of Naval Research 800 North Quincy Street Arlington, Virginia 22217	1

ABSTRACTS DISTRIBUTION LIST, 056/625/629

Dr. G. A. Somorjai
Department of Chemistry
University of California
Berkeley, California 94720

Dr. J. Murday
Naval Research Laboratory
Surface Chemistry Division (6170)
455 Overlook Avenue, S.W.
Washington, D.C. 20375

Dr. J. B. Hudson
Materials Division
Rensselaer Polytechnic Institute
Troy, New York 12181

Dr. Theodore E. Madey
Surface Chemistry Section
Department of Commerce
National Bureau of Standards
Washington, D.C. 20234

Dr. J. E. Demuth
IBM Corporation
Thomas J. Watson Research Center
P.O. Box 218
Yorktown Heights, New York 10598

Dr. M. G. Lagally
Department of Metallurgical
and Mining Engineering
University of Wisconsin
Madison, Wisconsin 53706

Dr. R. P. Van Duyne
Chemistry Department
Northwestern University
Evanston, Illinois 60637

Dr. J. M. White
Department of Chemistry
University of Texas
Austin, Texas 78712

Dr. D. E. Harrison
Department of Physics
Naval Postgraduate School
Monterey, California 93940

Dr. W. Kohn
Department of Physics
University of California, San Diego
La Jolla, California 92037

Dr. R. L. Park
Director, Center of Materials
Research
University of Maryland
College Park, Maryland 20742

Dr. W. T. Peria
Electrical Engineering Department
University of Minnesota
Minneapolis, Minnesota 55455

Dr. Keith H. Johnson
Department of Metallurgy and
Materials Science
Massachusetts Institute of Technology
Cambridge, Massachusetts 02139

Dr. S. Sibener
Department of Chemistry
James Franck Institute
5640 Ellis Avenue
Chicago, Illinois 60637

Dr. Arold Green
Quantum Surface Dynamics Branch
Code 3817
Naval Weapons Center
China Lake, California 93555

Dr. A. Wold
Department of Chemistry
Brown University
Providence, Rhode Island 02912

Dr. S. L. Bernasek
Department of Chemistry
Princeton University
Princeton, New Jersey 08544

Dr. P. Lund
Department of Chemistry
Howard University
Washington, D.C. 20059

ABSTRACTS DISTRIBUTION LIST, 056/625/629

Dr. F. Carter
Code 6132
Naval Research Laboratory
Washington, D.C. 20375

Dr. Richard Colton
Code 6112
Naval Research Laboratory
Washington, D.C. 20375

Dr. Dan Pierce
National Bureau of Standards
Optical Physics Division
Washington, D.C. 20234

Dr. R. Stanley Williams
Department of Chemistry
University of California
Los Angeles, California 90024

Dr. R. P. Messmer
Materials Characterization Lab.
General Electric Company
Schenectady, New York 22217

Dr. Robert Gomer
Department of Chemistry
James Franck Institute
5640 Ellis Avenue
Chicago, Illinois 60637

Dr. Ronald Lee
R301
Naval Surface Weapons Center
White Oak
Silver Spring, Maryland 20910

Dr. Paul Schoen
Code 5570
Naval Research Laboratory
Washington, D.C. 20375

Dr. John T. Yates
Department of Chemistry
University of Pittsburgh
Pittsburgh, Pennsylvania 15260

Dr. Richard Greene
Code 5230
Naval Research Laboratory
Washington, D.C. 20375

Dr. L. Kesmodel
Department of Physics
Indiana University
Bloomington, Indiana 47403

Dr. K. C. Janda
California Institute of Technology
Division of Chemistry and Chemical
   Engineering
Pasadena, California 91125

Dr. E. A. Irene
Department of Chemistry
University of North Carolina
Chapel Hill, Northc Carolina 27514

Dr. Adam Heller
Bell Laboratories
Murray Hill, New Jersey 07974

Dr. Martin Fleischmann
Department of Chemistry
Southampton University
Southampton 509 5NH
Hampshire, England

Dr. John W. Wilkins
Cornell University
Laboratory of Atomic and
   Solid State Physics
Ithaca, New York 14853

Dr. Richard Smardzewski
Code 6130
Naval Research Laboratory
Washington, D.C. 20375

Dr. H. Tachikawa
Chemistry Department
Jackson State University
Jackson, Mississippi 39217

ABSTRACTS DISTRIBUTION LIST, 056/625/629

Dr. R. G. Wallis
Department of Physics
University of California
Irvine, California 92664

Dr. D. Ramaker
Chemistry Department
George Washington University
Washington, D.C. 20052

Dr. J. C. Hemminger
Chemistry Department
University of California
Irvine, California 92717

Dr. T. F. George
Chemistry Department
University of Rochester
Rochester, New York 14627

Dr. G. Rubloff
IBM
Thomas J. Watson Research Center
P.O. Box 218
Yorktown Heights, New York 10598

Dr. Horia Metiu
Chemistry Department
University of California
Santa Barbara, California 93106

Captain Lee Myers
AFOSR/NC
Bollig AFB
Washington, D.C. 20332

Dr. J. T. Keiser
Department of Chemistry
University of Richmond
Richmond, Virginia 23173

Dr. Roald Hoffmann
Department of Chemistry
Cornell University
Ithaca, New York 14853

Dr. R. W. Plummer
Department of Physics
University of Pennsylvania
Philadelphia, Pennsylvania 19104

Dr. E. Yeager
Department of Chemistry
Case Western Reserve University
Cleveland, Ohio 41106

Dr. N. Winograd
Department of Chemistry
Pennsylvania State University
University Park, Pennsylvania 16802

Dr. G. D. Stein
Mechanical Engineering Department
Northwestern University
Evanston, Illinois 60201

Dr. A. Steckl
Department of Electrical and
  Systems Engineering
Rensselaer Polytechnic Institute
Troy, NewYork 12181

Dr. G. H. Morrison
Department of Chemistry
Cornell University
Ithaca, New York 14853

Dr. P. Hansma
Physics Department
University of California
Santa Barbara, California 93106

Dr. J. Baldeschwieler
California Institute of Technology
Division of Chemistry
Pasadena, California 91125

Dr. W. Goddard
California Institute of Technology
Division of Chemistry
Pasadena, California 91125

ABSTRACTS DISTRIBUTION LIST, 056/625/629

Dr. J. E. Jensen
Hughes Research Laboratory
3011 Malibu Canyon Road
Malibu, California 90265

Dr. J. H. Weaver
Department of Chemical Engineering
  and Materials Science
University of Minnesota
Minneapolis, Minnesota 55455

Dr. W. Knauer
Hughes Research Laboratory
3011 Malibu Canyon Road
Malibu, California 90265

Dr. C. B. Harris
Department of Chemistry
University of California
Berkeley, California 94720

END

FILMED

7-85

DTIC